

Expression of osteoprotegerin from a replicating adenovirus inhibits the progression of prostate cancer bone metastases in a murine model

James J Cody^{1,*}, Angel A Rivera^{2,*†}, Gray R Lyons^{1,‡}, Sherry W Yang¹, Minghui Wang², Jason W Ashley¹, Sreelatha Meleth^{3,§}, Xu Feng¹, Gene P Siegal^{1,4,5} and Joanne T Douglas^{2,5}

Metastatic involvement of the skeleton is a frequent consequence of advanced prostate cancer. These skeletal metastases cause a number of debilitating complications and are refractory to current treatments. New therapeutic options are being explored, including conditionally replicating adenoviruses (CRADs). CRADs are engineered to selectively replicate in and destroy tumor cells and can be 'armed' with exogenous transgenes for enhanced potency. We hypothesized that a CRAD armed with osteoprotegerin (OPG), an inhibitor of osteoclastogenesis, would inhibit the progression of prostate cancer bone metastases by directly lysing tumor cells and by reducing osteoclast activity. Although prostate cancer bone metastases are predominantly osteoblastic in nature, increased osteoclast activity is critical for the growth of these lesions. Ad5- Δ 24-sOPG-Fc-RGD is a CRAD that carries a fusion of the ligand-binding domains of OPG and the Fc region of human IgG1 in place of the viral *E3B* genes. To circumvent low tumor cell expression of the native adenoviral receptor, an arginine-glycine-aspartic acid (RGD) peptide insertion within the viral fiber knob allows infection of cells expressing α_v integrins. A 24-base pair deletion (Δ 24) within viral E1A limits replication to cells with aberrant retinoblastoma cell cycle regulator/tumor suppressor expression. We have confirmed that Ad5- Δ 24-sOPG-Fc-RGD replicates within and destroys prostate cancer cells and, in both murine and human coculture models, that infection of prostate cancer cells inhibits osteoclastogenesis *in vitro*. In a murine model, progression of advanced prostate cancer bone metastases was inhibited by treatment with Ad5- Δ 24-sOPG-Fc-RGD but not by an unarmed control CRAD.

Laboratory Investigation (2013) 93, 268–278; doi:10.1038/labinvest.2012.179; published online 28 January 2013

KEYWORDS: adenovirus; bone metastasis; oncolytic virus; osteoprotegerin; prostate cancer; virotherapy

Advanced prostate cancer exhibits a propensity for metastasis to the skeleton, and thus a majority of patients with late-stage disease will be diagnosed with bone metastases.^{1,2} The growth of metastatic cells in bone disrupts normal bone physiology and structure³ and causes a range of serious complications, including pain, pathological fractures and spinal cord compression.^{2,4} Current treatments with surgery, radiotherapy, chemotherapy and bisphosphonate administration may slow disease progression, but are associated with deleterious side effects⁵ and are often not curative. In light

of the above, new therapies for this disease are urgently needed.

One new class of anticancer agents is comprised of conditionally replicating adenoviruses (CRADs) based upon human serotype 5.⁶ These are adenoviruses that have been engineered to selectively replicate within cancer cells, thereby amplifying the input dose of virus and destroying the infected tumor cells by lysis. Through multiple rounds of selective infection, replication, lysis and spread, CRADs have the potential to destroy tumors while sparing normal tissue.

¹Department of Pathology, The University of Alabama at Birmingham, Birmingham, AL, USA; ²Division of Human Gene Therapy, Departments of Medicine, Obstetrics and Gynecology, Pathology and Surgery, The University of Alabama at Birmingham, Birmingham, AL, USA; ³Division of Preventive Medicine, Department of Medicine, The University of Alabama at Birmingham, Birmingham, AL, USA; ⁴The Center for Metabolic Bone Disease Core Laboratory, The University of Alabama at Birmingham, Birmingham, AL, USA and ⁵The Gene Therapy Center, The University of Alabama at Birmingham, Birmingham, AL, USA

Correspondence: Dr GP Siegal, MD, PhD, Department of Pathology, Division of Anatomic Pathology, The University of Alabama at Birmingham, 508 20th Street South, HSB 149K, Birmingham, AL 35294, USA.

E-mail: gsiegal@uab.edu

*These authors contributed equally to this work.

[†]Present address: Department of Pediatrics, Division of Hematology and Oncology and The Gene Therapy Center, Emory University, Atlanta, GA, USA.

[‡]Present address: Medical Scientist Training Program, Duke University, Durham, NC, USA.

[§]Present address: Statistics and Epidemiology Division, Social Statistical and Environmental Sciences, RTI International, Atlanta, GA, USA.

Received 12 July 2012; revised 8 November 2012; accepted 29 November 2012

However, clinical trials have shown that while CRAds are safe to administer,⁷ their potency must be improved before the full potential of this treatment modality can be realized.

One strategy to increase the efficacy of a CRAd is to employ it as a platform for the delivery of a therapeutic transgene. Owing to viral replication, an 'armed' CRAd amplifies the input dose of the transgene and can exert an antitumor effect by multiple mechanisms of action. A variety of armed CRAds directed against a range of malignancies has been described, and it is clear that the inclusion of a rationally selected transgene enhances the potency of a CRAd.⁸ An armed CRAd intended for prostate cancer bone metastasis will therefore be most effective when it has been selected in consideration of tumor–bone interactions. Prostate cancer bone metastases involve a disruption of normal bone homeostasis and influence the bone microenvironment in ways that are not fully understood. Prostate cancer cells produce a variety of factors including bone morphogenetic proteins, endothelin 1, and insulin-like growth factors that induce the growth of lesions, which are predominantly osteoblastic in their behavior.⁹ However, both blastic and lytic processes are involved, and thus osteoclasts also contribute to lesion growth.¹⁰ Prostate cancer cells can mediate osteoclast formation both directly and indirectly,¹¹ largely through the interaction of receptor activator of NF- κ B ligand (RANKL) on osteoblasts with its receptor RANK on osteoclast precursors. It has been shown that blockade of the RANK/RANKL interaction inhibits the progression of prostate cancer bone metastases,¹² even those which are osteoblastic in nature.^{13,14} This interaction can be disrupted by the normal bone protein osteoprotegerin (OPG), which is a soluble decoy receptor for RANKL.^{15,16} OPG is secreted by osteoblasts and bone stromal cells as a key mediator of normal bone homeostasis; it prevents the binding of RANKL with RANK to inhibit osteoclast differentiation/activation and promote bone formation. Several studies have demonstrated that OPG inhibits the progression of prostate cancer bone metastases.^{13,17–21} We therefore hypothesized that a CRAd armed with OPG would reduce the growth of prostate cancer bone metastases by two means: direct lysis of tumor cells due to viral replication, and a reduction in tumor burden by the inhibition of osteoclastic bone resorption by OPG.

We have previously constructed and described the armed CRAd used in this study, designated Ad5- Δ 24-sOPG-Fc-RGD.²² Cancer-selective replication is conferred by means of a 24-base pair deletion in the *E1A* gene,²³ which yields a protein unable to bind and inactivate the retinoblastoma tumor suppressor/cell cycle regulatory protein and restricts efficient viral replication to neoplastic cells. To enhance tumor cell transduction, this armed CRAd also includes a fiber knob with an arginine–glycine–aspartic acid (RGD) peptide insertion in the HI loop.²⁴ This modification directs initial binding of the virus to $\alpha_v\beta_3$ and $\alpha_v\beta_5$ integrins, which

are involved in prostate cancer bone metastasis,^{25,26} and thus overcomes the deficiency of the native coxsackievirus and adenovirus receptor (CAR) on prostate cancer cells.²⁷ This armed CRAd carries a transgene encoding the RANKL-binding domains of OPG fused to the Fc portion of human IgG1. It therefore lacks the domains of OPG that bind tumor necrosis factor-related apoptosis-inducing ligand,²⁸ precluding its ability to act as a survival factor for prostate cancer cells.²⁹ We have previously shown that the expression of OPG-Fc does not alter the selectivity of replication of the parent CRAd in experiments involving normal human epithelial cells and human liver slices.²²

MATERIALS AND METHODS

Cells

The human prostate cancer cell lines LNCaP^{30,31} and PC3³² were purchased from the American Type Culture Collection (ATCC; Manassas, VA, USA). The human prostate cancer cell line C4-2B, a subline of LNCaP with enhanced propensity for bone metastasis, was a gift from Dr Leland Chung. ST2 murine bone marrow stromal cells³³ were from the Riken Cell Bank, Japan. ST2 cells were propagated in α -minimum essential medium (α -MEM) and both the LNCaP and PC3 prostate cancer cells were cultured in Roswell Park Memorial Institute (RPMI) 1640 medium. C4-2B cells were cultured in T-Medium (Invitrogen, Carlsbad, CA, USA). These media were supplemented with 10% (v/v) heat-inactivated fetal bovine serum (FBS; Invitrogen), L-glutamine (2 mM), penicillin (100 U/ml) and streptomycin (100 μ g/ml). All cell lines were cultured at 37 °C in a humidified atmosphere, with ST2 cells maintained at 8% CO₂ and all others at 5% CO₂. Except where otherwise noted, media and supplements were from Mediatech (Herndon, VA, USA).

A C4-2B cell subline that stably expresses luciferase (C4-2B-LUC) was generated by transduction of the cells with a lentiviral vector encoding the firefly luciferase gene, as follows. 293GPG cells were cultured in Dulbecco's Modified Eagle Medium supplemented with 10% (v/v) heat-inactivated FBS, tetracycline, puromycin, G418, and penicillin/streptomycin as described previously.³⁴ These cells were maintained exclusively in the laboratory of Xu Feng, Ph.D., in accordance with a materials transfer agreement. A plasmid, pMX-puro-Luc, was prepared by the insertion of firefly luciferase cDNA into the *Bam*HI and *Not*I restriction sites of the pMX-puro retroviral vector. Then, 293GPG cells were transiently transfected with this vector using Lipofectamine Plus reagent (Invitrogen). Virus supernatants were collected at 48, 72 and 96 h after transfection and then pooled. C4-2B cells were then infected with the viral supernatant for 24 h in the presence of 8 μ g/ml Polybrene (hexadimethrine bromide). The infection medium was then replaced with cell culture medium and cells were allowed to recover for 24 h before selection with 2 μ g/ml puromycin.

Viruses

The wild-type human adenovirus serotype 5, Adwt300, was purchased from ATCC. The tropism-modified control virus Ad5-RGD has wild-type E1 and E3 regions as well as an RGD peptide in the HI loop of the fiber knob and was previously generated in our laboratory.²² The two unarmed control CRAds used in this study, Ad5- Δ 24 and Ad5- Δ 24RGD, each have a 24-base pair deletion in the CR2 region of E1A and have been described previously.³⁵ The tropism-modified control CRAd, Ad5- Δ 24RGD, also has an RGD peptide in the HI loop of the fiber knob. The two armed CRAds used in this study, Ad5- Δ 24-sOPG-Fc and Ad5- Δ 24-sOPG-Fc-RGD, each carry a transgene encoding the RANKL-binding domains of human OPG (amino acids 1-201¹⁵) fused to the Fc portion of human IgG1.²⁸ The transgene is in place of the E3B region of the genome, under native expression control elements. The construction of these CRAds, as well as that of the E1-deleted replication-deficient control vectors Ad-CMV-sOPG-Fc-RGD and Ad-CMV-OPG-Fc-RGD, which expresses full-length OPG, has been detailed previously.²²

Expression of sOPG and Viral Genes

Monolayers of C4-2B cells in 24-well plates were infected with Ad5- Δ 24-sOPG-Fc, Ad5- Δ 24-sOPG-Fc-RGD or Adwt300 at a multiplicity of infection (MOI) of 0.1 infectious units (IU) per cell in RPMI 1640 with 2% (v/v) FBS. Cells were incubated for 1 h at 37 °C before the infection mixtures were removed and replaced with serum-free growth medium with supplements. At various intervals post infection (4, 8, 12, 24 and 36 h), medium was collected, and cell lysates were harvested by the addition of buffer RLT (RNeasy Mini Kit; Qiagen, Valencia, CA, USA) to the wells. Samples were stored at -80 °C until they could be further processed.

Total cellular RNA was isolated from lysate samples using an RNeasy Mini Kit (Qiagen), according to the manufacturer's instructions. Purified RNA samples were then subjected to real-time quantitative reverse transcriptase PCR analysis using a LightCycler 480 system (Roche Diagnostics, Indianapolis, IN, USA). Samples from cells infected with the armed CRAds were assayed for the expression of sOPG-Fc, whereas samples from cells infected with Adwt300 were assayed for the expression of the E3B genes 14.7k and RID β (primer sequences previously published).²² All samples were analyzed for the expression of E3 gp19k, adenovirus death protein (ADP) and fiber. The expression of human glyceraldehyde-3-phosphate dehydrogenase was used as a control. Results are expressed as copy number/ng of total RNA.

Secretion of sOPG-Fc

Monolayers of LNCaP and C4-2B cells in 24-well plates were infected with Ad5- Δ 24-sOPG-Fc or Ad5- Δ 24-sOPG-Fc-RGD as above, before the infection mixtures were removed and replaced with serum-free growth medium with supplements. Medium samples were collected at various intervals post

infection (24, 36, 48 and 60 h) and stored at -80 °C. After the final time point, samples were thawed and concentrated to 1/10 of the original volume using a Microcon centrifugal filter device (Millipore, Bedford, MA, USA) and centrifuged at 14 000 \times g. The presence of sOPG-Fc was determined by SDS-PAGE followed by immunoblotting using a goat anti-human OPG primary antibody (Sigma-Aldrich, St Louis, MO, USA) diluted 1:1000 and a rabbit anti-goat alkaline phosphatase-conjugated secondary antibody (Jackson ImmunoResearch, West Grove, PA, USA), diluted 1:4000. Blots were developed with 5-bromo-4-chloro-3-indolyl phosphate/nitro blue tetrazolium (Sigma-Aldrich).

Viral DNA Replication in Cell Lines

Monolayers of C4-2B cells in 24-well plates were infected with Adwt300, Ad5- Δ 24, Ad5- Δ 24RGD, Ad5- Δ 24-sOPG-Fc or Ad5- Δ 24-sOPG-Fc-RGD at an MOI of 0.1 IU per cell. At 2, 4 and 6 days post infection, 200 μ l samples of medium were collected and stored at -20 °C until further processing. DNA was then purified from the medium samples using a QIAamp DNA Blood Mini Kit (Qiagen). Samples were analyzed by quantitative real-time PCR on a LightCycler 480 system (Roche Diagnostics) for the presence of the Ad5 *E4* gene (primer sequences previously published²²), as an indicator of viral replication.³⁶ Results are expressed as copy number/ng of total DNA.

Cytopathic Effect

To assay oncolytic potency qualitatively, monolayers of C4-2B, LNCaP and PC3 cells in 24-well plates were infected with Ad5- Δ 24-sOPG-Fc-RGD and each of the replicating control viruses at MOIs of 1, 0.1 and 0.01 IU per cell. After 8 days, the viability of the cells was determined by staining the monolayers with 1% (w/v) crystal violet (Fisher Scientific) in 70% (v/v) ethanol for 1 h. Plates were washed in tap water to remove excess dye.

Osteoclast Formation

The ability of the armed CRAds to inhibit osteoclast formation was assayed in both murine and human cells, using *in vitro* osteoclastogenesis assays that are detailed elsewhere and summarized here.^{22,33} In the murine system, bone marrow macrophages were isolated from 4- to 8-week-old female athymic nude Foxn1^{nu} mice (Harlan, Indianapolis, IN, USA) and cocultured in a 10:1 ratio with ST2 murine bone marrow stromal cells in α -MEM containing 10% (v/v) FBS, 1×10^{-8} M 1,25-dihydroxyvitamin D3 (Biomol Research Laboratories, Plymouth Meeting, PA, USA) and 1×10^{-6} M dexamethasone (Sigma-Aldrich). After a 24 h recovery phase, porous (0.4 μ m pore size) Transwell inserts 12 mm in diameter (Corning; Corning, NY, USA) containing monolayers of C4-2B cells that had been infected immediately before transfer at an MOI of 0.1 IU per cell with each of the CRAds or Ad-CMV-OPG-Fc-RGD, diluted in RPMI 1640 with 2% (v/v) FBS for 1 h, were added to these

cocultures. Cultures were maintained in α -MEM supplemented with 10% (v/v) FBS, 1×10^{-8} M 1,25-dihydroxyvitamin D3 and 1×10^{-6} M dexamethasone.

In the human system, bone marrow macrophages were isolated from fresh human bone marrow purchased from Lonza (Lonza Walkersville, Walkersville, MD, USA) and prepared as previously described.³⁷ These cells were plated in 24-well plates and cultured in α -MEM containing 10% FBS (v/v) supplemented with 10 ng/ml macrophage colony-stimulating factor and 25 ng/ml recombinant human RANKL (R&D Systems) for 48 h to allow attachment. Then, monolayers of C4-2B cells cultured on porous (0.02 μ m pore size) 10 mm diameter Anopore inserts (Nalge Nunc International; Rochester, NY, USA), which had been infected immediately before transfer with each of the CRAds or Ad-CMV-sOPG-Fc-RGD, as above, were transferred to the 24-well plates. The cultures were maintained in α -MEM containing 10% FBS (v/v) supplemented with macrophage colony-stimulating factor and RANKL.

The cocultures were maintained in their respective osteoclastogenic media, with conditioned medium being collected from each well and replaced with 1 ml fresh medium every 3 days. At the completion of each experiment, the inserts carrying prostate cancer cells were stained with crystal violet. Samples of conditioned medium from day 9 were assayed for the presence of the osteoclast-specific protein tartrate-resistant acid phosphatase 5b³⁸ as an indicator of osteoclast formation, using a MouseTRAP or BoneTRAP ELISA kit (Immuno-diagnostic Systems, Fountain Hills, AZ, USA) for murine and human osteoclasts, respectively.

Murine Model of Prostate Cancer Bone Metastasis

Animal experiments were conducted in accordance with federal and institutional guidelines for animal care. Osteoblastic lesions were established by the injection of 5×10^5 C4-2B-LUC cells into the left tibiae of 4- to 5-week-old male Fox Chase SCID beige mice (Harlan).³⁹ Cells were prepared for injection by detachment with Versene followed by two washes in phosphate buffered saline (PBS) and a final resuspension in PBS at 2.5×10^7 cells/ml. Aliquots of 20 μ l (5×10^5 cells) of single cell suspension were loaded into BD Micro-Fine IV needle (28 G) insulin syringes (3/10 cc; BD Consumer Healthcare, Franklin Lakes, NJ, USA), which were kept on ice until the animals were ready for injection. Forty-five mice were anesthetized with 2% (v/v) isoflurane (MWI, Meridian, ID, USA) gas at a flow rate of 0.5-1 l/min per mouse and were injected with cells in the proximal end of the left tibia. After 33 weeks, the mice were randomly divided into three treatment groups. Mice from two treatment groups were given intratibial injections of 2×10^6 IU of either Ad5- Δ 24-sOPG-Fc-RGD ($n=7$) or Ad5- Δ 24RGD ($n=7$) in a total volume (TV) of 20 μ l of PBS. The third group of animals was injected with PBS only ($n=6$). Three weeks after treatment, the mice were killed, as were three additional age-matched

control naïve mice. The left tibia of each was dissected and preserved in 10% (w/v) neutral buffered formalin (Fisher Scientific).

Tomography

For the determination of the 3D architecture of the trabecular bone, mouse tibiae were analyzed by micro computed tomography (μ CT), using a Scanco μ CT40 desktop cone-beam scanner (Scanco Medical AG, Brüttisellen, Switzerland). Tibiae were placed vertically in 12 mm diameter scanning holders. Scans were performed at the following settings: 6 μ m resolution, 70 kVp, 114 μ A with an integration time of 200 ms. Scans were automatically reconstructed into 2D slices, and the region of interest was outlined in each slice using the μ CT Evaluation Program (v5.0A, Scanco Medical).

The scan of the trabecular bone was performed below the growth plate, and each scan consisted of 209 slices, of which 100 were used for analysis. A region of interest was drawn on each of the 100 slices just inside the cortical bone, to include only the trabecular bone and marrow. Trabecular bone was thresholded at 247, to distinguish it from the marrow. The 3D reconstruction was performed on the region of interest which only contained trabecular bone; no cortical bone was present in these regions of interest. Data were obtained on TV of the scanned area, the volume of trabecular bone (BV) within that area, BV/TV, trabecular bone density, trabecular number, separation and thickness.

Statistical Analysis

Student-Fisher *t*-tests were used to analyze data from *in vitro* osteoclast formation assays. For the tomography data, a Kruskal-Wallis test was used as a non-parametric alternative to ANOVA, to examine overall differences between the four groups. As all outcomes were marginally or highly significant overall, pairwise comparisons between groups were done via Wilcoxon two-sample tests to identify outcomes that were significantly different between treatments. There was no adjustment for multiple testing as these are hypothesis-generating experiments. In all analyses, differences were considered significant when $P \leq 0.05$.

RESULTS

Characterization of a Tropism-Modified, sOPG-Fc-armed CRAd in Prostate Cancer Cells

The genomes of the viruses used in this study are depicted in Figure 1. Ad5- Δ 24-sOPG-Fc-RGD is a tropism-modified CRAd that expresses an sOPG-Fc fusion gene from the E3B region of the adenovirus genome. The sOPG-Fc transgene replaces the native *E3B* genes (RID α , RID β and 14.7k) and was placed under native gene expression control elements. This CRAd retains expression of the E3-11.6k ADP for efficient lysis of infected cells and includes an RGD-modified fiber knob for enhanced transduction of tumor cells, as well as a Δ 24-modified *E1A* gene for cancer-selective replication. An sOPG-Fc-armed CRAd with native tropism,

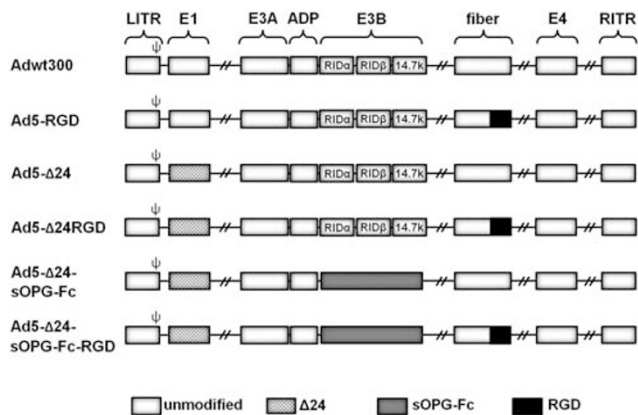


Figure 1 The genomes of the viruses used in this study are represented schematically. By convention, the adenovirus genome is depicted as having (from left to right): a left inverted terminal repeat (LITR) containing the packaging signal (ψ), the early 1 (*E1*) gene, *E3A* region, ADP, *E3B* region (containing the receptor internalization and degradation alpha (*RID α*), *RID β* and 14.7k genes), fiber gene, *E4* gene, and right inverted terminal repeat (RITR). For clarity, additional adenoviral genes are not shown. Modifications made to specific viruses, as indicated, include a 24-base pair deletion within *E1* ($\Delta 24$), replacement of *E3B* with an sOPG-Fc fusion gene and the inclusion of a RGD peptide within the knob domain of the fiber.

Ad5- $\Delta 24$ -sOPG-Fc, was included as a control for infectivity. Other control viruses included Ad5- $\Delta 24$ and Ad5- $\Delta 24$ -RGD, unarmed CRAds with native and modified tropism, respectively. Ad5-RGD is a tropism-modified control virus that is otherwise syngeneic with the wild-type adenovirus Adwt300.

In a previous study, we demonstrated in breast cancer cells that the expression of sOPG-Fc from a CRAd mimicked that of the replaced native *E3B* genes, in both timing and amount.²² Hence, we first wished to confirm these findings in prostate cancer cells. We selected for analysis the C4-2B cell line, which is a subline of LNCaP with an enhanced propensity for bone metastasis *in vivo*. C4-2B cells were infected with Ad5- $\Delta 24$ -sOPG-Fc, Ad5- $\Delta 24$ -sOPG-Fc-RGD or Adwt300, and cell lysates were analyzed by quantitative reverse transcriptase PCR at multiple time points post infection. The sOPG-Fc transgene was expressed late in the infection cycle, at levels similar to that of the 14.7 k gene from Ad300wt (Figure 2a). Also, the expression of ADP from Ad5- $\Delta 24$ -sOPG-Fc and Ad5- $\Delta 24$ -sOPG-Fc-RGD is similar to that from Adwt300 in both timing and amount (Figure 2b). Together, these data indicate that the sOPG-Fc transgene is efficiently expressed in prostate cancer cells in a manner consistent with its placement in the adenoviral genome, and that the expression of surrounding viral genes is not altered.

To confirm that prostate cancer cells infected with the armed CRAds secrete sOPG-Fc into the medium, monolayers of both LNCaP and C4-2B cells were infected with Ad5- $\Delta 24$ -sOPG-Fc-RGD or with Ad5- $\Delta 24$ -sOPG-Fc. At multiple time points post infection, samples of conditioned medium were subjected to immunoblotting with an OPG-specific primary

antibody. In samples from infected C4-2B cells, sOPG-Fc was detected in the medium beginning at 36 h post infection (Figure 2c). LNCaP cells released sOPG-Fc into the medium at 24 h and 36 h when infected with Ad5- $\Delta 24$ -sOPG-Fc-RGD or with Ad5- $\Delta 24$ -sOPG-Fc, respectively (Figure 2d). In both cell lines, sOPG-Fc protein increased in amount until 60 h post infection. These results confirm that prostate cancer cells infected with the armed CRAds efficiently secrete sOPG-Fc.

Expression of sOPG-Fc does not Enhance the Oncolytic Potency of a CRAd in Prostate Cancer Cells

We next sought to confirm that prostate cancer cells would support the replication of a CRAd armed with sOPG-Fc. Monolayers of C4-2B cells were infected with both the tropism-modified and -unmodified armed CRAds, their respective unarmed control CRAds, or with wild-type adenovirus. Conditioned medium was collected 2, 4 and 6 days post infection, and DNA isolated from the samples was analyzed by quantitative real-time PCR for the adenovirus *E4* gene, as an indicator of viral replication. Both of the sOPG-Fc-armed CRAds replicated efficiently in the C4-2B cells, at levels similar to the unarmed CRAds and Adwt300 (Figure 3a). Thus, it is evident that the expression of sOPG-Fc from a CRAd does not enhance adenoviral replication in prostate cancer cells. To determine whether the expression of sOPG-Fc inhibits the ability of a CRAd to efficiently lyse infected prostate cancer cells, a panel of prostate cancer cells was infected with Ad5- $\Delta 24$ -sOPG-Fc-RGD or control viruses. This panel included lines with low levels of CAR expression (C4-2B⁴⁰ and PC3⁴¹) as well as a line expressing high levels of CAR (LNCaP⁴²). After 8 days the monolayers were stained with crystal violet, in a qualitative assay for oncolytic potency. As indicated by the cleared wells resulting from viral oncolysis, all viruses were sufficiently potent to completely destroy the monolayers of each cell line at an MOI of 0.1 (Figure 3b). Although most viruses completely destroyed the monolayers at the lower MOI of 0.01, the tropism-modified armed CRAd exhibited reduced oncolytic potency in comparison with its unarmed control. This result indicates that the expression of OPG does not enhance the potency of an armed CRAd in prostate cancer cells *in vitro*. This is not unexpected, as our hypothesis predicts that the additional antitumor effect of OPG expression would be manifested only in the bone microenvironment. Considered together with the viral replication data, these experiments demonstrate that the expression of sOPG-Fc from a CRAd does not enhance viral replication or oncolytic potency in prostate cancer cells.

CRAds Armed with sOPG-Fc Inhibit Osteoclast Formation *in vitro*

Both murine and human cell culture systems were used to determine whether prostate cancer cells infected with the armed CRAds would inhibit osteoclast formation while simultaneously being lysed by viral replication. Monolayers

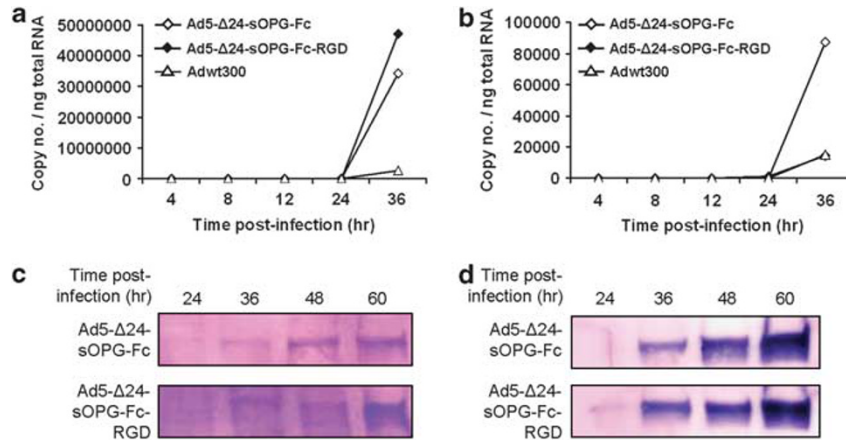


Figure 2 Characterization of armed CRAds. (a, b) C4-2B prostate cancer cells were infected with Ad5-Δ24-sOPG-Fc, Ad5-Δ24-sOPG-Fc-RGD or Adwt300. At the indicated times post infection, total cellular RNA was extracted and subjected to quantitative reverse transcriptase PCR to detect expression of: (a) the *sOPG-Fc* gene (for cells infected with Ad5-Δ24-sOPG-Fc or Ad5-Δ24-sOPG-Fc-RGD) or the *14.7k* gene (for cells infected with Adwt300); and (b) the *ADP* gene. (c, d) Secretion of sOPG-Fc by infected C4-2B (c) and LNCaP (d) cells. At the indicated times post infection, conditioned medium was collected and subjected to immunoblot analysis using an anti-OPG primary antibody.

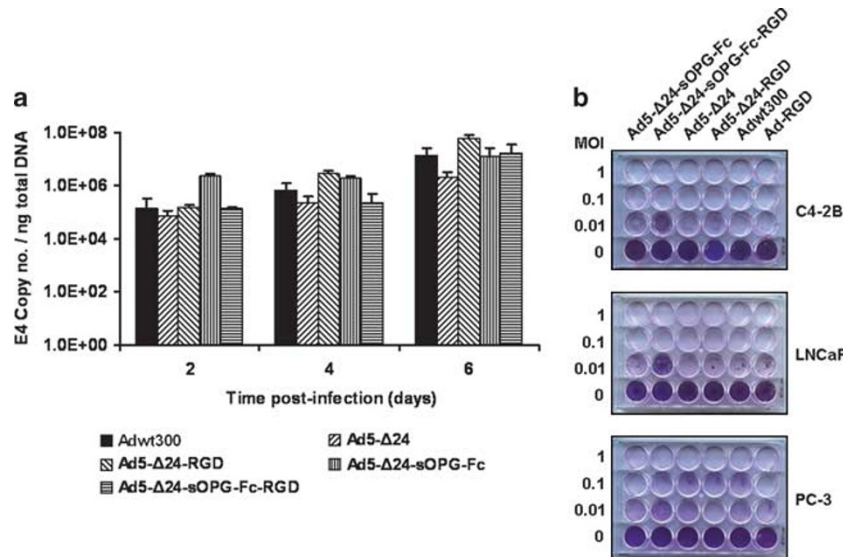


Figure 3 Oncolytic potency of the armed CRAds. (a) C4-2B prostate cancer cells were infected with Adwt300, Ad5-Δ24, Ad5-Δ24RGD, Ad5-Δ24-sOPG-Fc or Ad5-Δ24-sOPG-Fc-RGD. The conditioned culture medium was collected at 2, 4 and 6 days post infection. DNA was extracted and subjected to Q-PCR to detect the *E4* gene as a measure of viral DNA replication. Results are the means \pm s.d. of duplicate determinations. Representative results of three separate experiments are shown. (b) a panel of prostate cancer cell lines was infected at the indicated MOIs. Eight days post infection, viable cells were fixed and stained with crystal violet. Representative results of three separate experiments are shown.

of C4-2B cells were established on permeable cell culture inserts and then infected with the unarmed control CRAds, Ad5-Δ24 and Ad5-Δ24RGD, and both of the armed CRAds, Ad5-Δ24-sOPG-Fc or Ad5-Δ24-sOPG-Fc-RGD. Additional wells infected with tropism-modified, E1-deleted replication-deficient control vectors expressing OPG-Fc (murine experiment) or sOPG-Fc (human experiment) from the CMV promoter were included as controls for viral replication. The cell culture inserts containing the infected cells were then added either to cocultures of murine bone marrow macrophages and ST2 bone marrow stromal cells, or to cultures of

human bone marrow macrophages in recombinant soluble RANKL-containing medium. In both experiments, cultures were maintained in osteoclastogenic medium and thus were expected to form osteoclasts within 7–10 days. On day 9, conditioned medium samples were analyzed by an ELISA for the osteoclast-specific protein TRAP5b as an indicator of osteoclast formation. In both the murine (Figure 4a) and the human (Figure 4b) experiments, wells containing armed CRAds with either tropism-modified or wild-type fibers inhibited the formation of osteoclasts relative to their respective unarmed control CRAd platforms ($P < 0.05$ for all

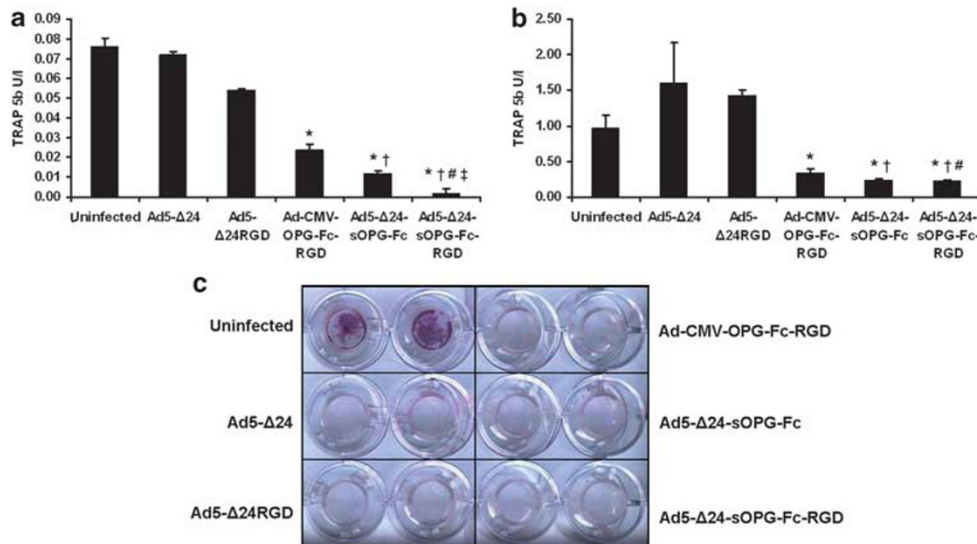


Figure 4 CRAds armed with sOPG-Fc simultaneously lyse prostate cancer cells and inhibit osteoclast formation *in vitro*. C4-2B cells were infected with the indicated adenoviruses and grown on inserts overlaying cocultures of murine osteoclast precursors and ST2 bone marrow stromal cells (a) or human osteoclast precursors and RANKL (b). At day 9, an ELISA was performed to detect TRAP5b, an osteoclast marker protein. Results are means \pm s.d. of duplicate determinations. Significant differences ($P < 0.05$) versus uninfected (*), unarmed CRAd (†), non-replicative vector (#), and armed CRAd with native tropism (‡) are indicated. Representative results of two separate experiments are shown. (c) Viable prostate cancer cells on the inserts were fixed and stained with crystal violet.

pairwise comparisons) or to the replication-defective vectors. In addition, Ad5-Δ24-sOPG-Fc-RGD inhibited the formation of osteoclasts to a greater extent than did Ad5-Δ24-sOPG-Fc in the murine cell coculture ($P < 0.05$). The monolayers containing the C4-2B cells were stained with crystal violet to assay cell viability. As shown for the murine experiment in Figure 4c, the cells were destroyed by the CRAds, indicating that tumor cell lysis occurs simultaneously with suppression of osteoclast formation. Overall, these findings support our hypothesis that an sOPG-Fc-armed CRAd can inhibit the growth of prostate cancer bone metastases by directly lysing tumor cells and by blocking the formation of osteoclasts.

A Tropism-Modified CRAd Armed with sOPG-Fc Inhibits Prostate Cancer Bone Metastasis *in vivo*

We next wished to demonstrate that the tropism-modified, armed CRAd, Ad5-Δ24-sOPG-Fc-RGD, could inhibit the growth of prostate cancer bone metastases *in vivo* more effectively than its unarmed control CRAd, Ad5-Δ24RGD. Osteoblastic bone metastases were established in male SCID beige mice by the injection of C4-2B-LUC cells into the left tibiae. Subsequently, a subset of mice developed rapidly growing tumors that impaired locomotion and were removed from the study in accordance with institutional regulations. The remaining mice developed slow-growing tumors, which became palpable at ~ 9 weeks and continued to increase in size over the duration of the study. In this experiment, tumor size did not correlate with bioluminescence quantification, and thus the imaging was not continued. After 33 weeks, the

mice were randomly divided into three cohorts and treated by the intratibial delivery of Ad5-Δ24RGD or Ad5-Δ24-sOPG-Fc-RGD or given PBS only as a control. Three weeks following treatment, the mice were killed and the tibiae were collected and analyzed by μ CT. The tibiae of three additional age-matched naïve mice were also collected and examined as examples of normal bone. The average ratio of trabecular bone volume to the total analyzed volume (BV/TV), surface area of trabecular bone and the density of the trabecular bone for each treatment group were then determined from the μ CT data.

Mice in the PBS and Ad5-Δ24RGD treatment groups exhibited a loss of trabecular bone, whereas mice treated with Ad5-Δ24-sOPG-Fc-RGD displayed a trabecular structure which more closely resembled that of the naïve control mice. Images of representative tibiae from each treatment group are shown in Figure 5. Comparison of group averages revealed a number of trends. Whereas naïve mice had a BV/TV ratio of 0.0644, mice treated with PBS had ratio of 0.0223 and those treated with Ad5-Δ24RGD had a ratio of 0.0246, representing decreases of 65 and 62%, respectively (Figure 6a). In contrast, the BV/TV ratio of Ad5-Δ24-sOPG-Fc-RGD treated mice (0.0496) was double that of the PBS and Ad5-Δ24RGD groups, and had decreased only 23% vs the naïve group. Similarly, as shown in Figure 6b, mice treated with the armed CRAd displayed a trabecular bone surface area, which more closely resembled the naïve mice (2.6982 vs 3.1104 mm²) than did that of the PBS- (1.5437 mm²) or Ad5-Δ24RGD-treated mice (1.37 mm²). Although the observed trends did not reach statistical

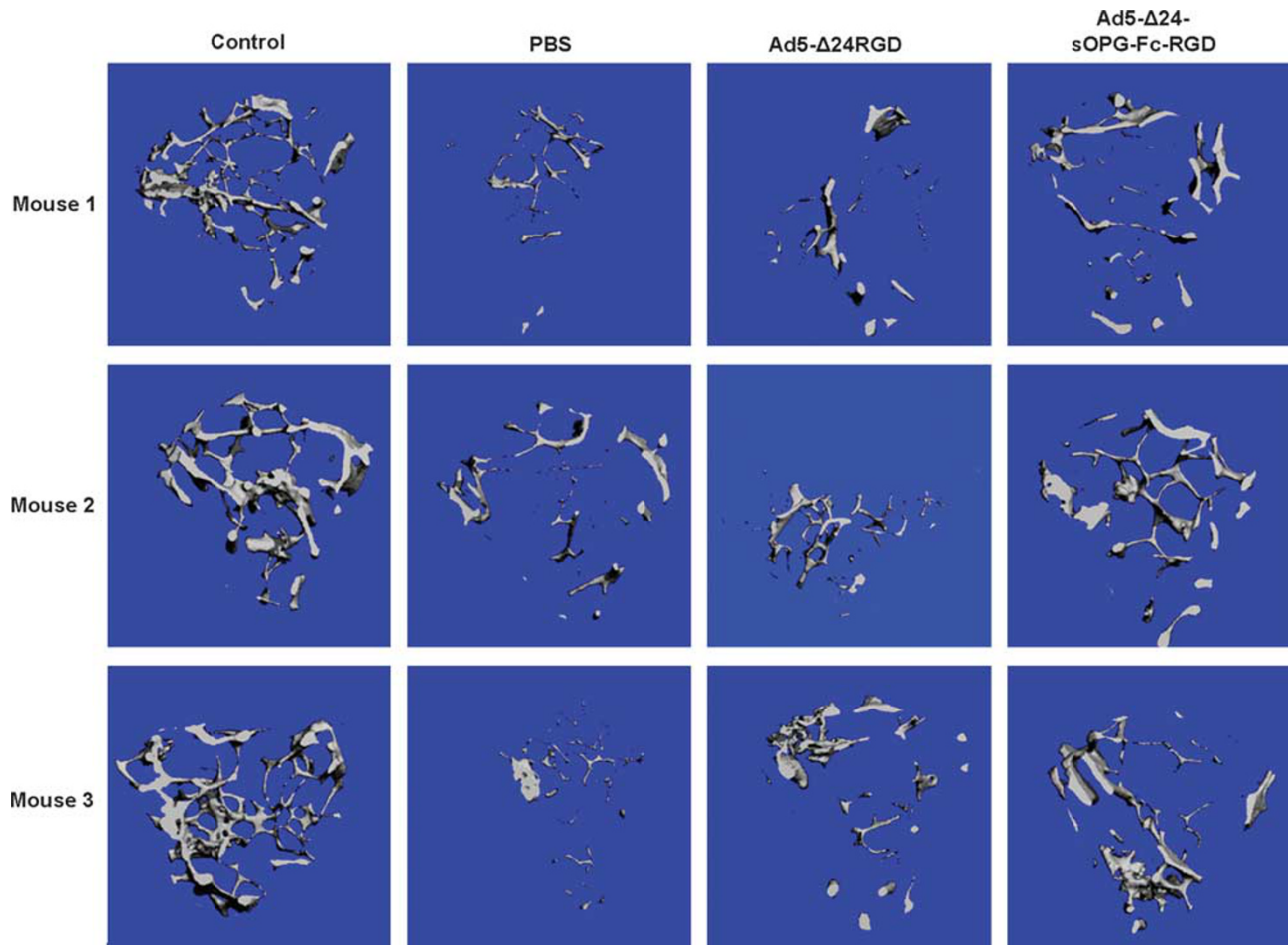


Figure 5 An sOPG-Fc-armed CRAAd inhibits the progression of bone metastases of prostate cancer *in vivo* more effectively than does an unarmed CRAAd. Intratibial tumors of C4-2B-LUC prostate cancer cells were established in SCID mice and treated with either Ad5-Δ24-sOPG-Fc-RGD, Ad5-Δ24RGD or PBS. Shown are μ CT images of the proximal tibiae of three naïve control mice and three representative mice from each treatment group.

significance by Wilcoxon Two-Sample analysis, similar findings were also observed in the examination of trabecular bone density (not shown).

In aggregate, these data show that a CRAAd armed with sOPG-Fc inhibits the progression of prostate cancer bone metastases and preserves normal bone architecture more effectively than does an unarmed control CRAAd, but further titration of experimental conditions will need to be performed to maximize clinical efficacy.

DISCUSSION

We have designed an armed CRAAd for bone metastases that targets both the metastatic tumor cell and the bone micro-environment. Prostate cancer commonly metastasizes to the skeleton^{1,2} where it relies on increased osteoclast activity.^{10,11} Thus, we hypothesized that an sOPG-Fc-armed CRAAd would be effective against this disease. Here, we have confirmed that sOPG-Fc is expressed and secreted from prostate cancer cells infected with Ad5-Δ24-sOPG-Fc-RGD, and that viral replication and tumor cell lysis are not enhanced by this

expression. We showed that Ad5-Δ24-sOPG-Fc-RGD inhibits osteoclastogenesis while simultaneously lysing prostate cancer cells. Finally, we have shown that Ad5-Δ24-sOPG-Fc-RGD more effectively controls the growth of established bone lesions *in vivo* than does Ad5-Δ24RGD, by more effectively preserving the normal bone architecture. Altogether, these results supported our hypothesis that a CRAAd armed with OPG can inhibit the growth of prostate cancer bone metastases by directly lysing tumor cells and by reducing osteoclast formation and activation.

We focused most of our studies on the C4-2B cell line, which is a bone metastatic derivative of the LNCaP line and establishes osteoblastic lesions *in vivo*.^{43,44} We also included for analysis LNCaP cells, which were derived from a lymph node metastasis, and PC3 cells, which were isolated from a bone metastasis. We observed similar levels of gene expression, viral replication and oncolytic potency between the tropism-modified and wild-type tropism CRAAds in these cell lines. The fact that each of these lines expresses CAR, with C4-2B⁴⁰ and PC3 cells⁴¹ expressing low but detectable levels

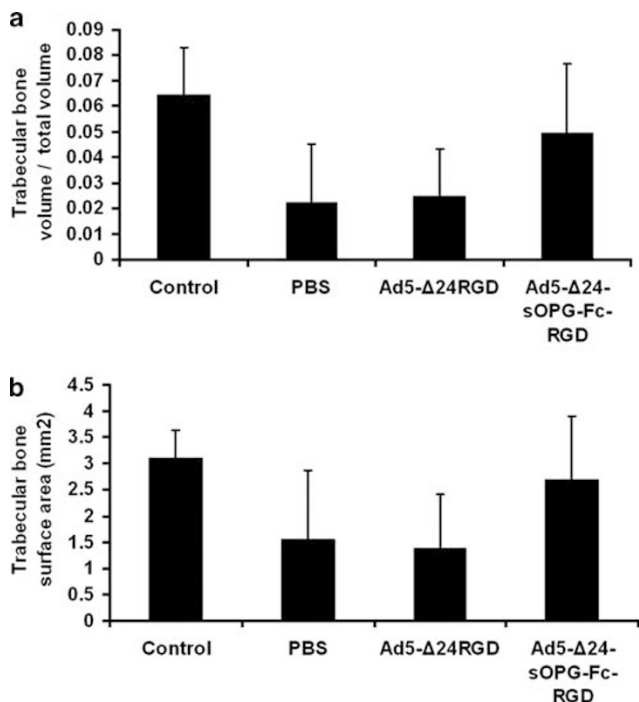


Figure 6 SCID mice bearing intratibial tumors of C4-2B-LUC were administered intratibial injections of Ad5-Δ24-sOPG-Fc-RGD, Ad5-Δ24RGD or PBS and were compared to naïve controls. Tibiae were collected and subjected to μ CT. Analysis of μ CT images was performed to determine the ratio of TV to trabecular bone volume (a) and trabecular bone surface area (b). Shown are the group means \pm s.d., $n=3$ (control), 6 (PBS), 7 (Ad-Δ24RGD) and 7 (Ad-Δ24-sOPG-Fc-RGD).

and LNCaP cells expressing high levels⁴² may explain these results. Although our *in vitro* experiments did not show a clear advantage in the use of the tropism-modified armed CRAd over its wild-type fiber control, a study by Rauen *et al* showed that the expression of CAR in prostate tumors is inversely correlated with tumor stage/aggressiveness.²⁷ Interestingly, CAR was detected in the four bone metastasis specimens analyzed, but expression was not uniform. Regardless, the RGD tropism modification does not preclude binding of the virus to CAR.²⁴ Therefore, the RGD-modified armed CRAd, with its expanded tropism, would likely be a more effective therapeutic than an isogenic CRAd with wild-type fibers. In our osteoclastogenesis experiments, cell death was observed in C4-2B cells infected with the non-replicative control vector. We speculate that this may have resulted from a toxic effect by some mechanism unrelated to replication; the reason for this cell death was not determined. Considered together with the oncolytic potency experiments, however, the data nonetheless show that an OPG-armed CRAd is capable of simultaneously destroying tumor cells by lysis while mediating an inhibition of osteoclastogenesis, consistent with our previous findings.²²

For our *in vivo* experiment, we developed a C4-2B cell line which stably expresses luciferase. Our intention was to monitor tumor growth non-invasively by bioluminescence imaging. However, tumor luciferase expression did not

correlate with tumor growth, and thus we were unable to rely upon imaging for tumor monitoring. This lack of correlation may have been due to the long time frame of the experiment, which may have allowed for a loss of luciferase expression. We observed the C4-2B tumors to be slow growing *in vivo*, which has been noted by others using this line.^{44–48} As in other intra-osseous murine models of prostate cancer bone metastases, progression is typically observed over periods of weeks to months, particularly in studies employing the LNCaP line and its derivatives.^{39,44,49–53} At the conclusion of our experiment, we observed extensive trabecular bone destruction rather than osteosclerosis, as indicated by an overall loss of trabecular bone in all treatment groups. This effect was also reported by Chanda *et al*, in a study demonstrating that intratibial tumors of C4-2B cells converted from an osteoblastic to an osteolytic phenotype after 6 months *in vivo*.⁴⁸ In a rat model of prostate cancer bone metastasis, Lynch *et al* showed that osteoclast numbers increased in mixed lesions up to 4 weeks, when the experiment was concluded.⁵⁴ This suggests that after an initial osteoblastic phase, the constant upregulation of osteoclast activity leads to an overall loss of bone in mature lesions. The biphasic growth of prostate cancer bone metastases may account for the contradictory roles of OPG in their development. Prostate cancer cell lines, including PC3, LNCaP²⁹ and C4-2B,⁵⁵ express OPG. This expression may promote tumor cell survival and bone formation initially, but is nonetheless insufficient to prevent the eventual loss of bone in mature lesions.

We intended to treat well-established tumors and therefore administered treatment at week 33. By treating established tumors, this was a more challenging model but one that more closely represented a clinical scenario. A variety of studies have examined the potential of OPG for the treatment of bone metastases of prostate cancer in murine models. These include studies in which OPG expression within a prostate cancer bone lesion inhibited both osteoblastic¹⁹ and osteolytic⁴⁸ tumor progression and others involving the use of recombinant OPG^{17,18,20,53,56} in intratibial models of prostate bone metastases. In these models, which include the osteolytic PC3 model^{14,20} and the osteoblastic LNCaP¹⁸ and C4-2B¹⁷ models, it has consistently been shown that the administration of recombinant OPG to tumor-bearing mice significantly reduces the growth of established intratibial lesions, but does not inhibit the growth of prostate cancer cells *in vitro* or the growth of subcutaneous xenografts. Two reports have implicated extracellular calcium in the growth of prostate cancer bone metastases,^{57,58} suggesting that the inhibition of bone resorption by factors such as OPG, by means of calcium depletion, may contribute to a reduction in prostate cancer bone metastasis. However, because OPG does not affect proliferation of prostate cancer cells, and is not directly cytotoxic, it is unlikely that OPG administration alone would be sufficient to eliminate established metastases. Regarding safety, it is possible that the expression of OPG

from a CRAd could influence the surrounding normal bone, with the most likely effect being a transient increase in bone formation. However, OPG was safely given to multiple myeloma and breast cancer patients in a Phase I trial.⁵⁹

For both tumor cell implantation and delivery of the CRAds, we utilized intratibial injection.³⁹ This method is frequently employed in models of prostate cancer bone metastasis, as systemic and orthotopic prostate cancer models do not efficiently establish bone metastases.^{44,60} This delivery method may have limited the antitumor effect that we were able to achieve, as the small size of the intratibial compartment limited the amount of virus that could be injected. Intratibial injection was a practical necessity, however, because the systemic delivery of adenovirus is unfeasible from a clinical standpoint, as intravenously delivered adenoviruses are largely sequestered by the liver.⁶¹ As work continues in the field of adenoviral targeting, this problem may be overcome in the future. In the μ CT analysis of the tumor-bearing tibiae, we observed a wide variability within treatment groups that prevented the observed trends from reaching statistical significance. This limitation of the intratibial tumor model has been reported by others.⁶² Although the observed trends were consistent across all measurements, larger treatment groups would have made statistical significance easier to attain. However, it is also likely that, due to inherently variable growth rates of tumors *in vivo*, unacceptably large numbers of mice might have been necessary, suggesting that better animal models are an additional requirement to move the field forward. Finally, this study was designed to examine certain end points. An expanded study in which samples are collected at specific time points to examine dynamic changes in viral replication and tumor/bone interactions would reveal valuable information that would guide the clinical application of this CRAd.

We have demonstrated the potential utility of an sOPG-Fc-armed CRAd as a treatment for prostate cancer bone metastases. A number of studies have been published regarding the use of oncolytic viruses for prostate cancer and have been reviewed by Fukuhara *et al.*⁶³ In particular, studies involving CRAds in models of prostate cancer bone metastasis,^{64,65} including one employing the C4-2B model⁶⁶ and one in which CRAds armed with a soluble transforming growth factor beta receptor II-Fc fusions are used in a PC3 model,⁶⁷ have underscored the potential for this treatment strategy. This report, however, is the first to evaluate an armed CRAd designed specifically for the bone micro-environment in a model of prostate cancer bone metastases. Furthermore, it is likely that this CRAd, Ad5- Δ 24-sOPG-Fc-RGD, will also be effective against other malignancies that metastasize to the skeleton such as lung, thyroid, or renal carcinomas.

ACKNOWLEDGEMENTS

We thank Xingsheng Li, and Maria S Johnson, at the Small Animal Bone Phenotyping Core facility in the UAB Center for Metabolic Bone Disease for

technical assistance with the μ CT analysis. This work was supported by National Institutes of Health Grants R01 CA108585 and T32 CA075930.

DISCLOSURE/CONFLICT OF INTEREST

The authors declare that equity in VectorLogics is held by JT Douglas.

1. Bubendorf L, Schopfer A, Wagner U, *et al.* Metastatic patterns of prostate cancer: an autopsy study of 1,589 patients. *Hum Pathol* 2000;31:578–583.
2. Coleman RE. Clinical features of metastatic bone disease and risk of skeletal morbidity. *Clin Cancer Res* 2006;12:6243s–6249ss.
3. Roudier MP, Vesselle H, True LD, *et al.* Bone histology at autopsy and matched bone scintigraphy findings in patients with hormone refractory prostate cancer: the effect of bisphosphonate therapy on bone scintigraphy results. *Clin Exp Metastasis* 2003;20:171–180.
4. Coleman RE. Metastatic bone disease: clinical features, pathophysiology and treatment strategies. *Cancer Treat Rev* 2001;27:165–176.
5. James ND, Bloomfield D, Luscombe C. The changing pattern of management for hormone-refractory, metastatic prostate cancer. *Prostate Cancer Prostatic Dis* 2006;9:221–229.
6. Alemany R, Balague C, Curiel DT. Replicative adenoviruses for cancer therapy. *Nat Biotechnol* 2000;18:723–727.
7. Kim D. Clinical research results with dl1520 (Onyx-015), a replication-selective adenovirus for the treatment of cancer: what have we learned? *Gene Ther* 2001;8:89–98.
8. Cody JJ, Douglas JT. Armed replicating adenoviruses for cancer virotherapy. *Cancer Gene Ther* 2009;16:473–488.
9. Mundy GR. Metastasis to bone: causes, consequences and therapeutic opportunities. *Nat Rev Cancer* 2002;2:584–593.
10. Roato I, D'Amelio P, Gorassini E, *et al.* Osteoclasts are active in bone forming metastases of prostate cancer patients. *PLoS One* 2008;3:e3627.
11. Inoue H, Nishimura K, Oka D, *et al.* Prostate cancer mediates osteoclastogenesis through two different pathways. *Cancer Lett* 2005;223:121–128.
12. Zhang J, Dai J, Yao Z, *et al.* Soluble receptor activator of nuclear factor kappaB Fc diminishes prostate cancer progression in bone. *Cancer Res* 2003;63:7883–7890.
13. Yonou H, Kanomata N, Goya M, *et al.* Osteoprotegerin/osteoclastogenesis inhibitory factor decreases human prostate cancer burden in human adult bone implanted into nonobese diabetic/severe combined immunodeficient mice. *Cancer Res* 2003;63:2096–2102.
14. Whang PG, Schwarz EM, Gamradt SC, *et al.* The effects of RANK blockade and osteoclast depletion in a model of pure osteoblastic prostate cancer metastasis in bone. *J Orthop Res* 2005;23:1475–1483.
15. Simonet WS, Lacey DL, Dunstan CR, *et al.* Osteoprotegerin: a novel secreted protein involved in the regulation of bone density. *Cell* 1997;89:309–319.
16. Udagawa N, Takahashi N, Yasuda H, *et al.* Osteoprotegerin produced by osteoblasts is an important regulator in osteoclast development and function. *Endocrinology* 2000;141:3478–3484.
17. Zhang J, Dai J, Qi Y, *et al.* Osteoprotegerin inhibits prostate cancer-induced osteoclastogenesis and prevents prostate tumor growth in the bone. *J Clin Invest* 2001;107:1235–1244.
18. Kiefer JA, Vessella RL, Quinn JE, *et al.* The effect of osteoprotegerin administration on the intra-tibial growth of the osteoblastic LuCaP 23.1 prostate cancer xenograft. *Clin Exp Metastasis* 2004;21:381–387.
19. Corey E, Brown LG, Kiefer JA, *et al.* Osteoprotegerin in prostate cancer bone metastasis. *Cancer Res* 2005;65:1710–1718.
20. Armstrong AP, Miller RE, Jones JC, *et al.* RANKL acts directly on RANK-expressing prostate tumor cells and mediates migration and expression of tumor metastasis genes. *Prostate* 2008;68:92–104.
21. Miller RE, Roudier M, Jones J, *et al.* RANK ligand inhibition plus docetaxel improves survival and reduces tumor burden in a murine model of prostate cancer bone metastasis. *Mol Cancer Ther* 2008;7:2160–2169.
22. Cody JJ, Rivera AA, Lyons GR, *et al.* Arming a replicating adenovirus with osteoprotegerin reduces the tumor burden in a murine model of osteolytic bone metastases of breast cancer. *Cancer Gene Ther* 2010;17:893–905.

23. Fueyo J, Gomez-Manzano C, Alemany R, *et al*. A mutant oncolytic adenovirus targeting the Rb pathway produces anti-glioma effect *in vivo*. *Oncogene* 2000;19:2–12.
24. Dmitriev I, Krasnykh V, Miller CR, *et al*. An adenovirus vector with genetically modified fibers demonstrates expanded tropism via utilization of a coxsackievirus and adenovirus receptor-independent cell entry mechanism. *J Virol* 1998;72:9706–9713.
25. Cooper CR, Chay CH, Pienta KJ. The role of alpha(v)beta(3) in prostate cancer progression. *Neoplasia* 2002;4:191–194.
26. Bisanz K, Yu J, Edlund M, *et al*. Targeting ECM-integrin interaction with liposome-encapsulated small interfering RNAs inhibits the growth of human prostate cancer in a bone xenograft imaging model. *Mol Ther* 2005;12:634–643.
27. Rauen KA, Sudilovsky D, Le JL, *et al*. Expression of the coxsackie adenovirus receptor in normal prostate and in primary and metastatic prostate carcinoma: potential relevance to gene therapy. *Cancer Res* 2002;62:3812–3818.
28. Emery JG, McDonnell P, Burke MB, *et al*. Osteoprotegerin is a receptor for the cytotoxic ligand TRAIL. *J Biol Chem* 1998;273:14363–14367.
29. Holen I, Croucher PI, Hamdy FC, *et al*. Osteoprotegerin (OPG) is a survival factor for human prostate cancer cells. *Cancer Res* 2002;62:1619–1623.
30. Horoszewicz JS, Leong SS, Chu TM, *et al*. The LNCaP cell line—a new model for studies on human prostatic carcinoma. *Prog Clin Biol Res* 1980;37:115–132.
31. Horoszewicz JS, Leong SS, Kawinski E, *et al*. LNCaP model of human prostatic carcinoma. *Cancer Res* 1983;43:1809–1818.
32. Kaighn ME, Narayan KS, Ohnuki Y, *et al*. Establishment and characterization of a human prostatic carcinoma cell line (PC-3). *Invest Urol* 1979;17:16–23.
33. Udagawa N, Takahashi N, Akatsu T, *et al*. The bone marrow-derived stromal cell lines MC3T3-G2/PA6 and ST2 support osteoclast-like cell differentiation in cocultures with mouse spleen cells. *Endocrinology* 1989;125:1805–1813.
34. Ory DS, Neugeboren BA, Mulligan RC. A stable human-derived packaging cell line for production of high titer retrovirus/vesicular stomatitis virus G pseudotypes. *Proc Natl Acad Sci USA* 1996;93:11400–11406.
35. Suzuki K, Alemany R, Yamamoto M, *et al*. The presence of the adenovirus E3 region improves the oncolytic potency of conditionally replicative adenoviruses. *Clin Cancer Res* 2002;8:3348–3359.
36. Rivera AA, Wang M, Suzuki K, *et al*. Mode of transgene expression after fusion to early or late viral genes of a conditionally replicating adenovirus via an optimized internal ribosome entry site *in vitro* and *in vivo*. *Virology* 2004;320:121–134.
37. Cody JJ, Rivera AA, Liu J, *et al*. A simplified method for the generation of human osteoclasts *in vitro*. *Int J Biochem Mol Biol* 2011;2:183–189.
38. Halleen JM, Alatalo SL, Suominen H, *et al*. Tartrate-resistant acid phosphatase 5b: a novel serum marker of bone resorption. *J Bone Miner Res* 2000;15:1337–1345.
39. Corey E, Quinn JE, Bladou F, *et al*. Establishment and characterization of osseous prostate cancer models: intra-tibial injection of human prostate cancer cells. *Prostate* 2002;52:20–33.
40. Kasman L, Onicescu G, Voelkel-Johnson C. Histone deacetylase inhibitors restore cell surface expression of the coxsackie adenovirus receptor and enhance CMV promoter activity in castration-resistant prostate cancer cells. *Prostate Cancer* 2012;2012:137163.
41. Pandha HS, Stockwin LH, Eaton J, *et al*. Coxsackie B and adenovirus receptor, integrin and major histocompatibility complex class I expression in human prostate cancer cell lines: implications for gene therapy strategies. *Prostate Cancer Prostatic Dis* 2003;6:6–11.
42. Seki T, Dmitriev I, Suzuki K, *et al*. Fiber shaft extension in combination with HI loop ligands augments infectivity for CAR-negative tumor targets but does not enhance hepatotropism *in vivo*. *Gene Ther* 2002;9:1101–1108.
43. Thalmann GN, Anezinis PE, Chang SM, *et al*. Androgen-independent cancer progression and bone metastasis in the LNCaP model of human prostate cancer. *Cancer Res* 1994;54:2577–2581.
44. Wu TT, Sikes RA, Cui Q, *et al*. Establishing human prostate cancer cell xenografts in bone: induction of osteoblastic reaction by prostate-specific antigen-producing tumors in athymic and SCID/bg mice using LNCaP and lineage-derived metastatic sublines. *Int J Cancer* 1998;77:887–894.
45. Hall CL, Bafico A, Dai J, *et al*. Prostate cancer cells promote osteoblastic bone metastases through Wnts. *Cancer Res* 2005;65:7554–7560.
46. Kitagawa Y, Dai J, Zhang J, *et al*. Vascular endothelial growth factor contributes to prostate cancer-mediated osteoblastic activity. *Cancer Res* 2005;65:10921–10929.
47. Rubin J, Fan X, Rahnert J, *et al*. IGF-I secretion by prostate carcinoma cells does not alter tumor-bone cell interactions *in vitro* or *in vivo*. *Prostate* 2006;66:789–800.
48. Chanda D, Isayeva T, Kumar S, *et al*. Therapeutic potential of adult bone marrow-derived mesenchymal stem cells in prostate cancer bone metastasis. *Clin Cancer Res* 2009;15:7175–7185.
49. Fizazi K, Yang J, Peleg S, *et al*. Prostate cancer cells-osteoblast interaction shifts expression of growth/survival-related genes in prostate cancer and reduces expression of osteoprotegerin in osteoblasts. *Clin Cancer Res* 2003;9:2587–2597.
50. Burton DW, Geller J, Yang M, *et al*. Monitoring of skeletal progression of prostate cancer by GFP imaging, X-ray, and serum OPG and PTHrP. *Prostate* 2005;62:275–281.
51. Yang M, Burton DW, Geller J, *et al*. The bisphosphonate olpadronate inhibits skeletal prostate cancer progression in a green fluorescent protein nude mouse model. *Clin Cancer Res* 2006;12:2602–2606.
52. Bonfil RD, Dong Z, Trindade Filho JC, *et al*. Prostate cancer-associated membrane type 1-matrix metalloproteinase: a pivotal role in bone response and intraosseous tumor growth. *Am J Pathol* 2007;170:2100–2111.
53. Morrissey C, Kostenuik PL, Brown LG, *et al*. Host-derived RANKL is responsible for osteolysis in a C4-2 human prostate cancer xenograft model of experimental bone metastases. *BMC Cancer* 2007;7:148.
54. Lynch CC, Hikosaka A, Acuff HB, *et al*. MMP-7 promotes prostate cancer-induced osteolysis via the solubilization of RANKL. *Cancer Cell* 2005;7:485–496.
55. Lin DL, Tarnowski CP, Zhang J, *et al*. Bone metastatic LNCaP-derivative C4-2B prostate cancer cell line mineralizes *in vitro*. *Prostate* 2001;47:212–221.
56. Quinn JE, Brown LG, Zhang J, *et al*. Comparison of Fc-osteoprotegerin and zoledronic acid activities suggests that zoledronic acid inhibits prostate cancer in bone by indirect mechanisms. *Prostate Cancer Prostatic Dis* 2005;8:253–259.
57. Li X, Liao J, Park SI, *et al*. Drugs which inhibit osteoclast function suppress tumor growth through calcium reduction in bone. *Bone* 2011;48:1354–1361.
58. Liao J, Schneider A, Datta NS, *et al*. Extracellular calcium as a candidate mediator of prostate cancer skeletal metastasis. *Cancer Res* 2006;66:9065–9073.
59. Body JJ, Greipp P, Coleman RE, *et al*. A phase I study of AMG-0007, a recombinant osteoprotegerin construct, in patients with multiple myeloma or breast carcinoma related bone metastases. *Cancer* 2003;97:887–892.
60. Singh AS, Figg WD. *In vivo* models of prostate cancer metastasis to bone. *J Urol* 2005;174:820–826.
61. Glasgow JN, Everts M, Curiel DT. Transductional targeting of adenovirus vectors for gene therapy. *Cancer Gene Ther* 2006;13:830–844.
62. Canon JR, Roudier M, Bryant R, *et al*. Inhibition of RANKL blocks skeletal tumor progression and improves survival in a mouse model of breast cancer bone metastasis. *Clin Exp Metastasis* 2008;25:119–129.
63. Fukuhara H, Homma Y, Todo T. Oncolytic virus therapy for prostate cancer. *Int J Urol* 2010;17:20–30.
64. Matsubara S, Wada Y, Gardner TA, *et al*. A conditional replication-competent adenoviral vector, Ad-OC-E1a, to cotarget prostate cancer and bone stroma in an experimental model of androgen-independent prostate cancer bone metastasis. *Cancer Res* 2001;61:6012–6019.
65. Sandberg L, Papareddy P, Silver J, *et al*. Replication-competent Ad11p vector (RCAd11p) efficiently transduces and replicates in hormone-refractory metastatic prostate cancer cells. *Hum Gene Ther* 2009;20:361–373.
66. Li Y, Kacka M, Thompson M, *et al*. Conditionally replicating adenovirus therapy utilizing bone sialoprotein promoter (Ad-BSP-E1a) in an *in vivo* study of treating androgen-independent intraosseous prostate cancer. *Urol Oncol* 2011;29:624–633.
67. Hu Z, Gupta J, Zhang Z, *et al*. Systemic delivery of oncolytic adenoviruses targeting transforming growth factor- β inhibits established bone metastasis in a prostate cancer mouse model. *Hum Gene Ther* 2012;8:871–882.